

Atomic and electronic structure of Fe films grown on Pd{001}

J. Quinn, Y. S. Li, H. Li, D. Tian, and F. Jona

College of Engineering and Applied Science, State University of New York, Stony Brook, New York 11794

P. M. Marcus

IBM Research Center, P.O. Box 218, Yorktown Heights, New York 10598

(Received 31 August 1990)

The atomic and electronic structure of Fe films grown on Pd{001} is investigated by means of low-energy electron diffraction and angle-resolved photoemission spectroscopy (ARPES). The films grow pseudomorphically, probably by way of nucleation and growth of flat islands, which ultimately coalesce to form continuous Fe{001} films. The structure of these continuous films, if grown at slow rates (of the order of 0.1 Å/min), is body-centered tetragonal and is shown to be a distortion from the stable bcc structure of Fe: the in-plane lattice constant is 2.75 Å, as dictated by the Pd{001} substrate, and the bulk interlayer spacing is 1.50–1.53 Å. In 10–12-layer films the first interlayer spacing is expanded by 3.6% above bulk, but with increasing thickness that spacing contracts progressively to about 6.3% below the bulk value in 40–50-layer films. Films as thick as 60–70 layers can be grown pseudomorphically at slow rates despite the large misfit (4.2%) between bcc Fe{001} and fcc Pd{001}. ARPES data indicate that these films are electronically indistinguishable from bulk bcc Fe. Thick (about 200-layer) films grown at fast rates are essentially bcc, with in-plane lattice constants of 2.87 Å, but with slightly expanded (3%) interlayer spacing, attributed to the presence of carbon impurities.

I. INTRODUCTION

The iron-palladium system is interesting on the one hand because palladium has the tendency to become magnetically “active” in the presence of magnetic ions,¹ and on the other hand because the 4.2% misfit between bcc Fe ($a_0 = 2.87$ Å) and fcc Pd ($a_0 = 3.89$ Å, $a = 2.75$ Å, where a is the side of the primitive surface mesh, and the –8.4% misfit between fcc Fe ($a_0 = 3.59$ Å) and Pd make the occurrence of epitaxy in this system both ambiguous and complex.

Submonolayer Fe films on Pd{111} were grown and studied by Binns *et al.*¹ with low-energy electron diffraction (LEED) and Auger-electron spectroscopy (AES). The growth mode was classified as not simple and changed significantly with substrate temperature, but epitaxy was reportedly achieved for the first two atomic layers, with in-plane relaxation beginning in the third layer. Photoemission studies of the 3s core-level splitting seems to indicate that a flat monolayer of Fe on Pd{111} was paramagnetic with a local moment of $1.2\mu_B$, but small coverages in the second layer appeared to induce ferromagnetic order, while at approximately two-layer coverages the films appeared to “pass through an antiferromagnetic phase.”¹

On Pd{001}, however, Fe deposits reportedly exhibit submonolayer ferromagnetism. Liu and Bader^{2,3} used the surface magneto-optical Kerr effect (SMOKE) to establish that Fe films grown at 300 K are ferromagnetic already at the monolayer level, with magnetization parallel to the surface, while films grown at 100 K have magnetization perpendicular to the surface for thicknesses up to three layers, and parallel to the surface for larger

thicknesses. The growth mode was reported to be layer by layer on the basis of AES measurements, and films as thick as nine layers could be grown. It was assumed that the structure of Fe films on Pd{001} was a body-centered-tetragonal (bct) distortion of the fcc Fe phase.²

We present here the results of an extensive LEED, AES, and photoemission study of the atomic and electronic structure of Fe on Pd{001}, which show significant differences from previous work. Section II is concerned with experimental details and qualitative observations, Sec. III describes the quantitative LEED studies, Sec. IV describes the photoemission experiments, and Sec. V contains the conclusions.

II. EXPERIMENTAL DETAILS AND QUALITATIVE OBSERVATIONS

The experiments described below were carried out sequentially in two different chambers in two different laboratories with two different Fe sources. We will refer below to one set of experiments as HL, because the experiments were carried out in the home laboratory, and to the other set as U7, because the experiments were carried out at beamline U7 of the National Synchrotron Light Source.

A. Cleaning procedures—collection of LEED and photoemission data

After the preliminary cleaning operation described elsewhere,⁴ the Pd{001} surface was routinely cleaned *in situ* with sequences of argon-ion bombardments (375 V, 2 μA , 5×10^{-5} Torr, sample at room temperature) followed by anneals (about 775 °C for 30 min). The chemical state

of the surface was monitored by means of AES, carried out with the LEED optics as a retarding-field analyzer (RFA) for HL, or with a cylindrical mirror analyzer (CMA) for U7. An initial S impurity was eliminated by argon-ion bombardment of the surface at 550 °C for about 2 h. Despite the absence of any impurity signal from the AES spectrum, LEED initially gave an indication of very small residual contamination of the surface through the presence of extremely weak $c(2 \times 2)$ reflections that were visible only at electron energies lower than 50 eV. After several cycles of ion bombardments and anneals, these reflections disappeared and the LEED pattern from the Pd{001} surface was 1×1 , sharp, and with low background at all electron energies used—a direct indication of the absence of C from the surface region.⁴

Two types of LEED intensity data were studied in this work and are discussed below, namely spot profiles and integrated intensities. Both types were collected with a video-LEED combination of TV camera and microcomputer as described elsewhere.⁵

The photoemission experiments were done at the Beamline U7 of the National Synchrotron Light Source, featuring a plane-grating monochromator. The photoemission data were collected with a cylindrical mirror analyzer that was modified to allow angle-resolved experiments with an angular resolution of 2° as well as angle-integrated experiments. The samples were mounted on a newly designed manipulator that allows translations and rotations along three mutually perpendicular axes, as described elsewhere.⁶

B. Deposition of Fe

Iron was deposited on a clean Pd{001} surface (either at room temperature or cooled to about 120 K) from sources made with ultrapure (99.9995%) Fe platelets wrapped in Ta foil and heated electrically to about 1200 °C in the HL experiments, or from sources made with 99.999% pure Fe wires premelted on W wire in the U7 experiments. In the HL experiments, several impurities were codeposited on the Pd surface together with the iron, namely Cl, N, O, and C. Chlorine and nitrogen could be eliminated by outgassing the source at 1200 °C for about 24 h, and oxygen and carbon impurities were reduced by prolonged outgassing of the source, but they could never be eliminated completely from the AES spectra of the sample after exposure to the hot Fe source. The concentrations of impurities, as well as other properties of the Fe deposits, were found to depend on whether the deposition rate was slow or fast (these terms will be quantified below). In the U7 experiments the concentrations of impurities were smaller, as is discussed below.

In the HL experiments, for slow depositions the ratios of the oxygen AES line at 512 eV, and of the carbon AES line at 275 eV, to the Fe AES line at 651 eV were $I_{O_{512}}/I_{Fe_{651}} \approx 0.066$ (about 2.5 at. %), according to the formulas given in Ref. 7) and $I_{C_{275}}/I_{Fe_{651}} \approx 0.13$ (about 11 at. %), respectively. For fast depositions the ratios increased to about 0.24 (about 7%) for oxygen and 0.31 (about 22%) for carbon. In the U7 experiments, the ratios were $I_C/I_{Fe} = 0-0.02$ (0-2 at. %) for both slow and

fast rates, and $I_O/I_{Fe} = 0.15$ (about 6%) for slow and 0.22 (about 8%) for fast rates. It should be mentioned that all the ratios quoted here were measured on Fe films thick enough for the 330-eV Pd signal to disappear from the AES spectra.

The thicknesses of the Fe deposits were determined from the ratio $R = I_{Fe(651)}/I_{Pd(330)}$ between the intensities of the Fe and Pd AES lines at 651 and 330 eV, respectively, with the formula

$$R = R_0 \frac{1 - e^{-d/\lambda_{651}}}{e^{-d/\lambda_{330}}}, \quad (1)$$

where $R_0 = I_{Fe(651)}^\infty / I_{Pd(330)}^\infty = 0.13$ (as measured with the RFA) or 0.25 (as measured with the CMA); I^∞ denotes the intensity of the AES line from a very thick sample of Fe (Pd) at 651 (330) eV; and the λ 's are the inelastic mean free paths of electrons with 651 (330) eV energy traveling in Fe.

Equation (1) is obviously based on the assumption that the deposits are distributed uniformly over the area interrogated by the primary AES electron beam, i.e., that the films grow layer by layer—an assumption that in the present case may not be correct (see below). We use Eq. (1) anyway, but with the understanding that with it we calculate the thickness d of a uniform Fe layer that would produce the same R value as measured experimentally. This thickness is then converted to an equivalent number of Fe layers by assuming an interlayer spacing of 1.5 Å (as indicated by the LEED analysis presented below) and is quoted in units of layer equivalents, abbreviated LE.

The main difficulty with the use of Eq. (1), however, is that the values of the inelastic mean free path λ are not known very reliably. Table I lists the values of λ available in the literature for the electron energies used here. (Note that when using the LEED optics as a RFA one must correct the value of λ for the solid angle subtended by the optics, i.e., multiply λ of 0.84.) This uncertainty in the values of the inelastic mean free paths introduces an uncertainty of a factor of about 3 in the thickness d of the Fe deposits. Thus, typical *slow* deposition rates in the present work were either about 0.13 Å/min (as calculated with the high λ values) or about 0.05 Å/min (as calculated with the low λ values). We elected to use the values of λ suggested by Tanuma *et al.*⁸ for the calculations of equivalent layer thickness, but since the resolution of the controversy about the values of λ is not available at this time, we also listed in Table I the “multiplier” by which the LE's given in this paper should be multiplied in order to obtain the LE's that would be calculated with the other sets of λ 's given in Table I. In any case, it may be important for the discussion that follows to mention that the Pd signal disappeared from the AES spectra when the nominal thickness of the Fe films exceeded about 30 LE.

Thus, for depositions on the room-temperature substrate, *slow* rates in this paper means rates ranging from 0.05 to 0.13 Å/min, while *fast* rates were larger by about a factor of 100, i.e., about 10 Å/min or higher on the average. On the cooled substrate (about 120 K) the same electric power into the Fe source produced rates that were three times faster than on the unheated substrate,

TABLE I. λ_{330} and λ_{651} are the inelastic mean free paths of 330- and 651-eV electrons as reported by the authors listed in the first column. DR is the experimental deposition rate as calculated with the λ values listed on the same row. The film thicknesses quoted in this paper in LE have been calculated with the λ values listed in the first row. Multiplication of the quoted thickness values by the number listed in the last column produces the thicknesses that would be obtained with the λ values in the same row. The asterisk denotes the value for 350-eV Auger electrons from Ag traveling in Fe.

Authors	λ_{330} (Å)	λ_{651} (Å)	DR (Å/min)	Multiplier
TPP ^a	11.0	12.5	0.126	1
SD ^b	9.8	13.8	0.111	0.881
LB ^c	5.8	9.4	0.078	0.619
S <i>et al.</i> ^d	3.7*	8.2	0.050	0.397

^aTanuma, Powell, and Penn, Ref. 8.

^bSeah and Dench, Ref. 29.

^cLiu and Bader, Ref. 30.

^dSchneider *et al.*, Ref. 31.

i.e., 0.15–0.4 Å/min (presumably because of the increased sticking coefficient). In all cases, however, the film thicknesses quoted in this paper could be 50% larger or 50% smaller, depending on the applicable inelastic mean free path.

C. Mode of growth

We made several attempts to identify the mode of growth of the Fe films, in particular to determine whether the mode was layer by layer. We measured the profiles of the specular beam (at 8° angle of incidence) as functions of the Fe deposition at six different values of the incident electron energy, in an attempt to find the oscillations [analogous to the reflection high-energy electron-diffraction (RHEED) oscillations⁹] that allegedly characterize layer-by-layer growth.¹⁰ We also measured sequences of specular $I(V)$ spectra with increasing Fe deposition time in order to see whether oscillatory trends could be detected in the plot of the differences between successive $I(V)$ spectra *versus* deposition time.¹¹ Beyond a broad minimum in the latter plot we failed to find oscillations in any of the plots, and we therefore have no evidence for layer-by-layer growth in the present Fe/Pd system.

Thermodynamic arguments also speak against the possibility of layer-by-layer growth. The requirement for this growth mode to occur is that the sum of the film surface energy plus interfacial energy must be smaller than

TABLE II. Surface free-energy values (in J/m²) for Ag, Fe, and Pd as reported in the literature ($T_R=298.2$ K, T_M =melting point, $T_0=0$ K).

Authors	Ag	Pd	Fe
MG ^a (at T_R)	1.302	2.043	2.939
MG ^a (at T_M)	1.046	1.376	1.923
TM ^b (at T_M)	1.086	1.743	2.123
MCB ^c (at T_0)	1.250	2.100	2.550

^aMezey and Giber, Ref. 32.

^bTyson and Miller, Ref. 33.

^cMiedema, de Châtel, and de Boer, Ref. 34.

the substrate surface energy.¹² No information is available about the interface energy, but the fact that no intermixing of Fe and Pd at room temperature was detected either in previous epitaxy experiments^{1,2,3,13} or in the present ones (see Sec. III A) would seem to indicate that the interface energy term is positive. If we then assume that equilibrium conditions were approximated in our low-supersaturation (slow rates) experiments, the fact that the surface free energy of Fe is larger than that of Pd (see Table II) would seem to suggest that Fe is not likely to grow on Pd in the layer-by-layer mode, at least in the early stages.

D. LEED observations

The LEED pattern from clean Pd{001} remained 1×1 throughout all experiments with Fe deposition in this work, but the quality of the pattern, in particular the signal-to-noise ratio and the width of the diffracted beams, changed considerably with increasing Fe deposition. We describe the observations separately for the cases of slow and fast depositions.

1. Slow deposition: Substrate at room temperature

With increasing Fe deposition on the Pd{001} surface we observed a progressive worsening of the LEED pattern (increased background and broadened spots) up to thicknesses of 4 to 5 LE, but upon further deposition the pattern improved noticeably to the eye; while the quality never reached that of a clean Pd{001} pattern, the intensities of the beams and the overall contrast of the LEED pattern increased steadily up to about 20 LE. The FWHM (full width at half maximum) of the profile of the specular beam, as measured at 235 eV for 8° incidence, confirmed this visual observation. Figure 1 shows that the FWHM of the specular beam from films with a thickness of about 10 LE was the same as that from films with a thickness of about 3 LE. A qualitatively similar phenomenon has been reportedly observed on only one other epitaxial system so far, namely the system of Fe on Ag{001} (Ref. 14), and will be discussed further below.

Two other significant observations were made: (a) the Fe films could be grown to considerable thicknesses with

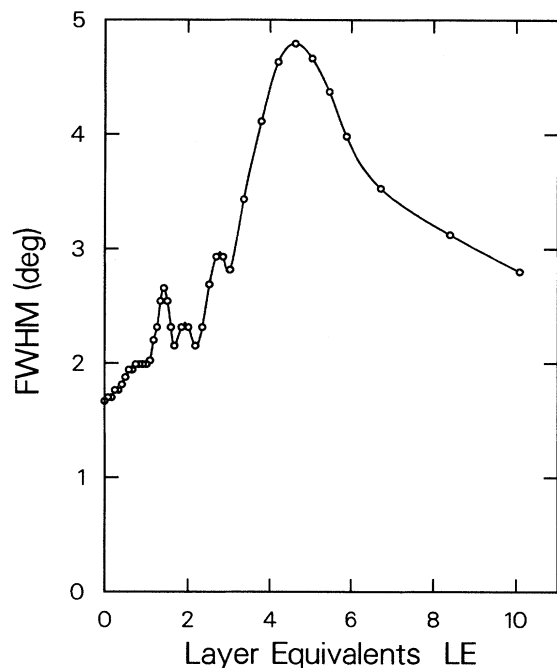


FIG. 1. Full width at half maximum (FWHM, in degrees) of the 00 beam, measured with 235-eV electrons at 8° incidence from Pd{001} increasingly covered with Fe, vs coverage. For reference, the angle between the 00 and the 10 beam was 17° .

the LEED pattern remaining 1×1 —the largest thickness reached in the present experiments was about 65 LE; and (b) the LEED $I(V)$ spectra changed gradually with film thickness up to about 40 LE and then remained unchanged from 40 to 65 LE. Figure 2 depicts a sequence of 11-beam $I(V)$ spectra for increasing coverage of Fe from 0 to 53 LE. This phenomenon is rather uncommon and will be discussed further below. It should be emphasized here that the LEED patterns from these very thick films were inferior in quality to that from clean and annealed Pd{001} in the sense that the background was higher and the spots were broader, but the signal-to-noise ratio was always large. Also, the quoted value of 65 LE for the maximum thickness attained should not be interpreted to mean that thicker films could not be grown, but only that deposition of Fe was stopped at that point.

2. Slow deposition: Substrate cooled to 120 K

The LEED patterns were noticeably sharper when the substrate was cooled to 120 K than when it was left unheated at room temperature. The phenomenon of first worsening and then successive improvement of the patterns is also observed at low temperatures, as described above. At any stage, the $I(V)$ spectra for equivalent coverages of the room-temperature and the low-temperature substrate, while not identical, were very similar to one another. Also, $I(V)$ spectra collected with the substrate at low temperature did not change when the substrate was warmed to room temperature. Overall, except for the improved sharpness of the LEED spectra, no

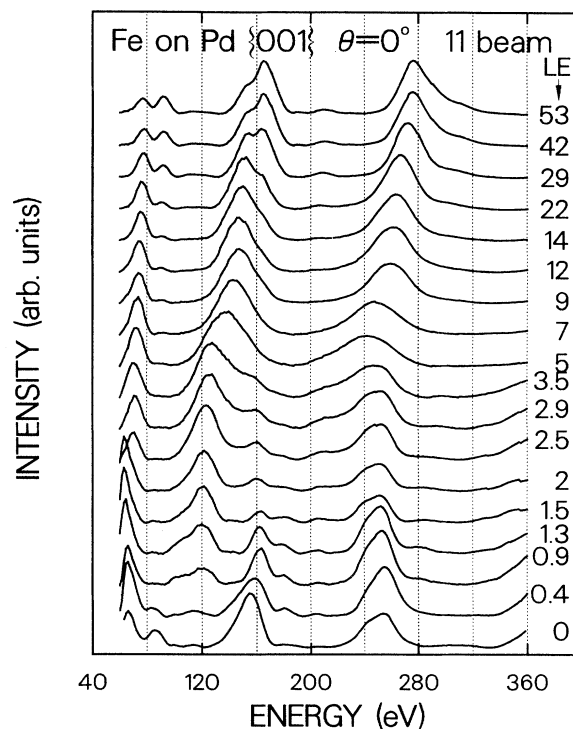


FIG. 2. Normal-incidence 11-beam LEED spectra for different coverages of Pd{001} by Fe.

significant differences were found between the phenomena observed with the substrate at low temperature and those observed with the room-temperature substrate.

3. Fast deposition

With fast-deposition rates we did not record the gradual evolution of the LEED $I(V)$ spectra with increasing thickness of the films as in Fig. 2, but we did study the thicker films. The thickest film grown in this work was estimated to be about 200 LE; the LEED pattern was noticeably worse than that of thick slowly grown films, but was always good enough for quantitative intensity data collection. Careful measurements revealed that the in-plane lattice constant was *larger* than that of the Pd{001} substrate, as will be discussed below.

III. QUANTITATIVE LEED STUDIES

The qualitative observations described above raise a number of questions about the crystallographic structure of the Fe films, whether grown by slow or fast deposition. To answer some of the questions, we have carried out quantitative intensity analyses of the LEED data and we report the results below. The intensity calculations were carried out with the CHANGE computer program;¹⁵ the Fe and Pd potentials were taken from the compilation of Moruzzi, Janak, and Williams;¹⁶ eight phase shifts and 69 beams were used for calculations up to 360 eV; the inner potential was initially chosen as $V_0 = -(10 + 4i)$ eV, with the real part treated as an adjustable parameter; and the

root-mean-square amplitude of the atomic vibrations was set at $\langle u^2 \rangle^{1/2} = 0.125 \text{ \AA}$. Evaluation of the correspondence between experiment and theory was done both visually and with reliability factors, namely R_{VHT} ,¹⁷ R_P ,¹⁸ and r_{ZJ} ,¹⁹ where VHT, P , and ZJ indicate Van Hove–Tong, Pendry, and Zanazzi–Jona factors, respectively. We discuss below the efforts made toward elucidation of the atomic structure in the early stages of growth, the results of the analyses of thick films grown by slow deposition, and the results of analyses of thick films grown by fast deposition.

A. Slow deposition—initial stages of growth

Despite visible worsening of the LEED pattern in the early stages of growth (primarily caused by higher background), LEED $I(V)$ spectra could be collected for several increasing coverages. The data were collected for normal incidence of the primary electron beam and included 19 degenerate spectra for a total (after averaging) of five nondegenerate spectra, namely 10, 11, 20, 21, and 22 at each coverage. As an example, several 11-type spectra are shown in Fig. 2. Already in the early stages these spectra are different from those of the clean Pd{001} surface, showing that the Fe atoms contribute not only to the background but also to the signal. This situation is different from the one encountered in the early stages of the growth of Fe on Ag{001},¹⁴ where the LEED $I(V)$ spectra were, despite the high background, practically identical to those of the clean substrate, showing that the Fe atoms did *not* contribute to the signal at that stage. Thus, in the present case the experiment tells us not only that the Fe atoms are ordered, but also that the units in which they are assembled have at least *some* flat {001} surfaces, and that these surfaces are epitaxial to the Pd{001} substrate.

The simplest explanation for this observation is, of course, that we may be looking at the early stages of layer-by-layer growth, despite our failed attempts at detecting it (as discussed in Sec. II C). Since one of the most convincing proofs for the existence of a pseudomorphic layer is a successful LEED structure determination, we calculated the LEED intensities expected from a single layer of Fe with the Pd{001} in-plane lattice constant and at a variable distance from the substrate (from 1.545 to 2.345 Å in steps of 0.1 Å). In view of the uncertainty in the thickness of the deposit (see Sec. II B), we were prepared to accept a fit to *any one* of the sets of $I(V)$ spectra collected in the early stages. We found no acceptable fit.

We then investigated other possible models of the surface structure, viz., (a) random intermixing of Fe and Pd in the first layer and in the first two layers, with either 25 at. % Pd–75 at. % Fe or 50:50 or 75:25, in all cases varying both the first interlayer spacing (d_{12}) and the second (d_{23}) between 1.545 and 2.345 Å; (b) single *underlayer* of Fe, with d_{12} varying between 1.445 and 1.945 Å and d_{23} between 1.745 and 2.145 Å; (c) bilayers of Fe over Pd, with d_{12} varying between 1.45 and 2.05 Å and d_{23} between 1.745 and 2.145 Å. All the results of these calculations were compared to all the experimental curves collected for nominal coverages between 0 and 5 LE. No ac-

ceptable fit was found.

These negative results do not exclude the possibility of complete Fe or Fe-Pd layers with structural parameters different from those tested. They do suggest, however, especially when considered in light of our failure to find evidence for layer-by-layer growth (Sec. II C), that layer-by-layer growth probably did not occur in our experiments. The fact that the LEED $I(V)$ spectra in the early stages are different (over the increased background) from those of the clean substrate may be explained by the existence of many small epitaxial flat-top Fe islands with different heights (producing, together with smaller and smaller areas of bare substrate surface, the increase in beam width predicted in Fig. 1), but such a model involves many fitting parameters (mainly the distribution function of island heights and the magnitudes of interlayer spacings), and was therefore not tested.

B. Slow deposition—thicker films

We now turn our attention to the fact that the LEED $I(V)$ spectra vary gradually with surface coverage even after the islands hypothesized above may be expected to have merged into continuous films (see, e.g., Fig. 2 for coverages above, say, 7 or 8 LE). This observation suggests that the atomic structure of the films changes gradually with thickness.

The first question that comes to mind is the following: does the lattice constant of the Fe films in the plane *parallel* to the substrate surface change with the thickness of the films? To answer this question we measured the intensity distribution on the LEED screen at a fixed energy (178 eV) along a $\langle 10 \rangle$ direction for both the clean Pd{001} surface and a 53-LE film of Fe. Contour plots and cross sections of these distributions are shown in Fig. 3 (center and top, respectively): it is clearly visible that the distances between the 02 and the $0\bar{2}$ beams are the same for clean Pd{001} as for the thick Fe film. Thus, the answer to the above question is negative: the films grown at slow rates have the same in-plane lattice constant (2.75 Å) as the Pd{001} surface within an error bound estimated at $\pm 1\%$ to $\pm 2\%$.

Since the in-plane lattice constant remains essentially the same during growth, the observed changes in the LEED $I(V)$ spectra indicate that the interlayer spacing is changing with thickness. The overall trend of the $I(V)$ curves above about 5 LE (see Fig. 2) is that the major peaks shift toward larger electron energies, suggesting a gradual contraction of interlayer spacings with increasing thickness up to about 40 LE; thereafter the $I(V)$ curves are stable. Thus, the second question that arises is the following: which interlayer spacing contracts, the bulk spacing or the surface spacing, or both?

We selected the 12-LE film and the 53-LE film for close quantitative scrutiny. The former produced a value of R [see Eq. (1)] of 0.8 and was selected because its nominal thickness corresponds to almost complete recovery of the LEED pattern after the initial worsening (cf. Fig. 1), thereby ensuring that the contribution of the Pd substrate to the LEED signal would be minimal. The 53-LE film was selected because it is well within the range of thicknesses that produce stable $I(V)$ spectra and its AES

spectrum showed no Pd signal at all (see Sec. II B).

The models chosen for intensity calculations involved semi-infinite Fe{001} crystals with variable bulk interlayer spacing (d_{bulk}), variable d_{12} , and variable d_{23} . Initially, d_{bulk} was varied, in steps of 0.1 Å, from 1.375 Å (the value appropriate for a bcc structure with $a_0=2.75$ Å, the lattice parameter of Pd{001}) through 1.945 Å (the value appropriate for a fcc structure with $a_0=3.89$, i.e., $a=2.75$) to 2.245 Å, in each case with d_{12} ranging from a contraction of 0.4 to an expansion of 0.4 Å. After promising correspondence with experiment was found in the vicinity of $d_{\text{bulk}} \approx 1.5$ Å, the refinement involved variations of d_{bulk} between 1.44 and 1.56 Å in steps of 0.03 Å, and of both d_{12} and d_{23} between compressions of 0.4 and expansions of 0.4 Å in steps of 0.05 Å.

The results of the refinements were as follows.

For the 12-LE film ($a_0=2.75$ Å),

$$d_{\text{bulk}} = 1.53 \pm 0.03 \text{ \AA} ,$$

$$\Delta d_{12} = +0.055 \pm 0.03 \text{ \AA} ,$$

$$\Delta d_{23} = +0.02 \pm 0.03 \text{ \AA} ,$$

$$R_{\text{VHT}} = 0.35, R_P = 0.58, r_{ZJ} = 0.13 .$$

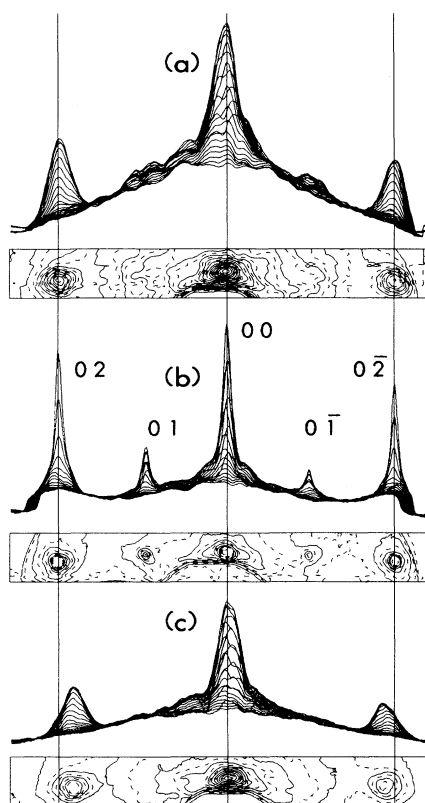


FIG. 3. LEED intensity distribution along a $\langle 10 \rangle$ direction in reciprocal space measured with 178-eV electrons at 5° incidence for (a) a thick (53 LE) slowly grown Fe film; (b) clean Pd{001}; (c) a thick (about 200 LE) fast-grown Fe film. The figures enclosed in rectangular frames are contour plots of the intensity, while the figures above them are cross sections depicting the beam profiles with the indices as indicated.

For the 53-LE film ($a_0=2.75$ Å),

$$d_{\text{bulk}} = 1.50 \pm 0.03 \text{ \AA} ,$$

$$\Delta d_{12} = -0.095 \pm 0.03 \text{ \AA} ,$$

$$\Delta d_{23} = -0.055 \pm 0.03 \text{ \AA} ,$$

$$R_{\text{VHT}} = 0.34, R_P = 0.59, r_{ZJ} = 0.14 .$$

The quality of the agreement between theory and experiment can be judged in Figs. 4 and 5.

Four comments about these results seem appropriate. First, we note that the gradual change observed in the experimental LEED $I(V)$ spectra with increasing thickness of the films (Fig. 2) is due primarily to increasing compressions of the first and second interlayer spacing, and only secondarily to a slight compression of the bulk interlayer spacing. Second, we confirm that the structure with "stable" LEED spectra of thick slowly grown Fe films (such as the 53-LE film) is bct, with $a_0=2.75$ Å (imposed by the Pd{001} substrate) and $c_0=3.0$ Å. We now ask whether this bct structure is a distortion from the structure of bcc α -Fe or from the structure of fcc γ -Fe? We can attempt to answer this question with strain analysis. The formula for this purpose was derived in Ref. 20, namely

$$\frac{(a_0 - a_e)/a_e}{(c_e - c_0)/c_e} = \frac{1 - \nu}{2\nu} , \quad (2)$$

where a_0 and c_0 are the lattice parameters of the film as grown, a_e and c_e are the lattice parameters of the undis-

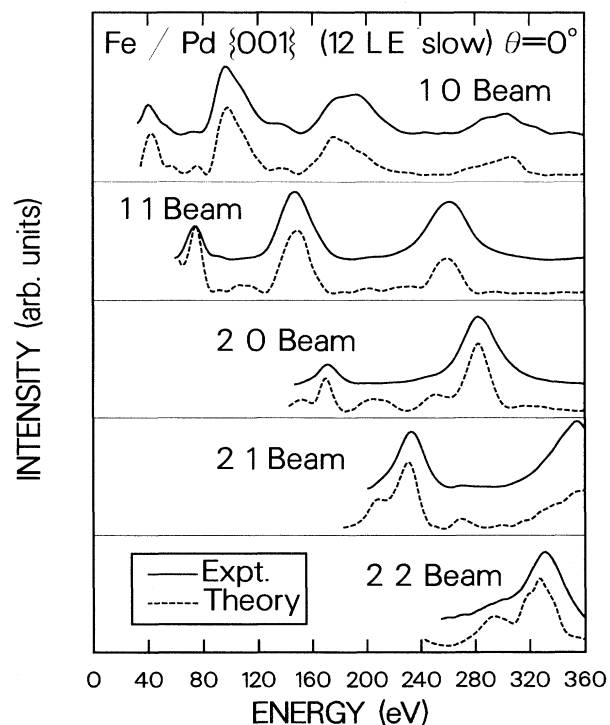


FIG. 4. Experimental and theoretical LEED spectra for a slowly grown 12-LE Fe film as described in the text.

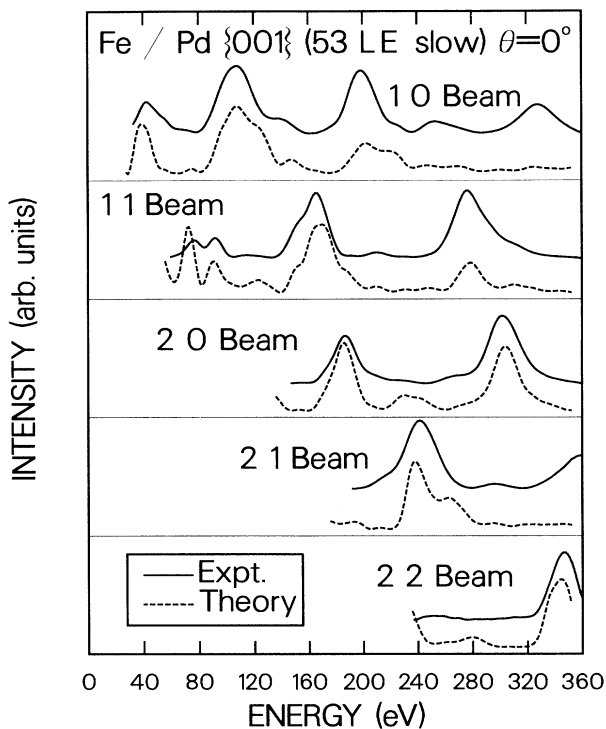


FIG. 5. Experimental and theoretical LEED spectra for a slowly grown 53-LE Fe film as described in the text.

torted (equilibrium) phase, and ν is Poisson's ratio. With $a_0 = 2.75 \text{ \AA}$, $c_0 = 3.0 \text{ \AA}$ we find, by assuming that the equilibrium phase is bcc α -Fe, i.e., $a_e = c_e = 2.87 \text{ \AA}$ (precisely 2.8664 \AA , Ref. 21), that $\nu = 0.35$, in good agreement with the value 0.37 obtained from precise measurements of the elastic constants of α -Fe.²² With $a_0 = 3.89 \text{ \AA}$, $c_0 = 3.0 \text{ \AA}$ we find, by assuming that the equilibrium phase is fcc γ -Fe, i.e., $a_e = c_e = 3.59 \text{ \AA}$ (Ref. 23), that $\nu = 0.5$ —the maximum possible value of Poisson's ratio. Although epitaxial films of γ -Fe were found to be elastically soft, with $\nu = 0.47$ (Ref. 23), it is very improbable that the equilibrium phase of the Fe films grown on Pd{001} is γ -Fe—the lattice misfit is -8.4% and the calculated Poisson ratio is too large. We conclude, therefore, that the equilibrium phase of the films grown in this work was bcc α -Fe. It is remarkable that films as thick as 65 LE and more can be grown, even with many defects and only with slow deposition rates, on a substrate with lattice misfit as large as 4.2% .

A third comment relates to the high concentration of carbon measured in the films grown in the HL experiments (see Sec. II B) and to the question of whether it could have affected the experimental results, since the LEED analyses were carried out with the HL data. Considering the fact that in the U7 experiments the concentration of C was much smaller, yet the results shown in Fig. 2 were reproduced satisfactorily, we do not believe that the presence of carbon in the grown films was responsible for the observed effects.

A final comment may be made on the phenomenon of contraction of the surface interlayer spacings with in-

creasing thickness of the films. In view of the theoretically established increase of atomic volume with magnetic moment,²⁴ we may speculate that the observed contractions are due to the decreasing magnetic moment of the surface Fe atoms. Theory predicts enhanced moments in ferromagnetic monolayers,^{25,26} and if the surface moments were to decrease gradually with increasing thickness, the phenomenon observed here would be at least qualitatively explained. We note, however, that the photoemission results, to be discussed below, offer no evidence for the hypothesis of varying magnetic moments in the surface region.

C. Fast deposition—thick films

As mentioned above, with deposition rates exceeding 4 LE/min we grew very thick films (about 200 LE), which produced LEED patterns of a quality inferior to that produced by thick slowly grown films, but still suitable for intensity measurements.

We concentrated first on the in-plane lattice constant. The LEED intensity distribution along $\langle 10 \rangle$ at 178 eV is compared to that measured on clean Pd{001} in Fig. 3 (center and bottom, respectively). It is obvious that, in contrast to the case of slowly grown thick films, the in-plane lattice constant of fast-grown thick films is larger than that of Pd{001}. Using the latter as reference and correcting for the off-center position of the sample in the LEED optics, we find that the in-plane lattice constant is $2.9 \pm 0.08 \text{ \AA}$. The large error (about 3%) in this case is attributed to the poor quality of the LEED pattern and the consequent imprecision in the determination of the maximum intensity in the broad diffracted beams. Nevertheless, it seems reasonable to conclude that the in-plane lattice constant of these films was that of the stable bcc α -phase of Fe (2.87 \AA)—the fast deposition rates must have facilitated the formation of misfit dislocations, which relieved the strain imposed by the substrate and allowed the growth, amid disorder and steps, of the unstrained phase.

However, quantitative intensity analysis shows that the LEED $I(V)$ spectra produced by these films are not matched well by calculations based on the stable bcc structure of Fe, even with variations of the first interlayer spacing d_{12} . It became necessary to vary the bulk interlayer spacing as well. The refinement yielded the best agreement with experiment with a model defined by $a_0 = 2.87 \text{ \AA}$, $d_{\text{bulk}} = 1.48 \text{ \AA}$, and $d_{12} = 1.48 \text{ \AA}$ (with $R_{\text{VHT}} = 0.25$, $R_P = 0.39$, and $r_{2J} = 0.10$). The agreement is not excellent, but it is better than for bcc Fe, as can be seen in Fig. 6, which juxtaposes experimental LEED spectra and those calculated for bcc and bct Fe as defined above.

Thus, we find that the fast-grown thick Fe films have a structure close to that of α -Fe, but exhibit an expansion of about 3% in the bulk interlayer spacing. This slight tetragonality is difficult to understand in films that are presumably free of strain. A possible explanation may be sought in the effect of the presence of considerable amounts of carbon that was measured on the surface of these films in the HL experiments, about 22 at. %, i.e.,

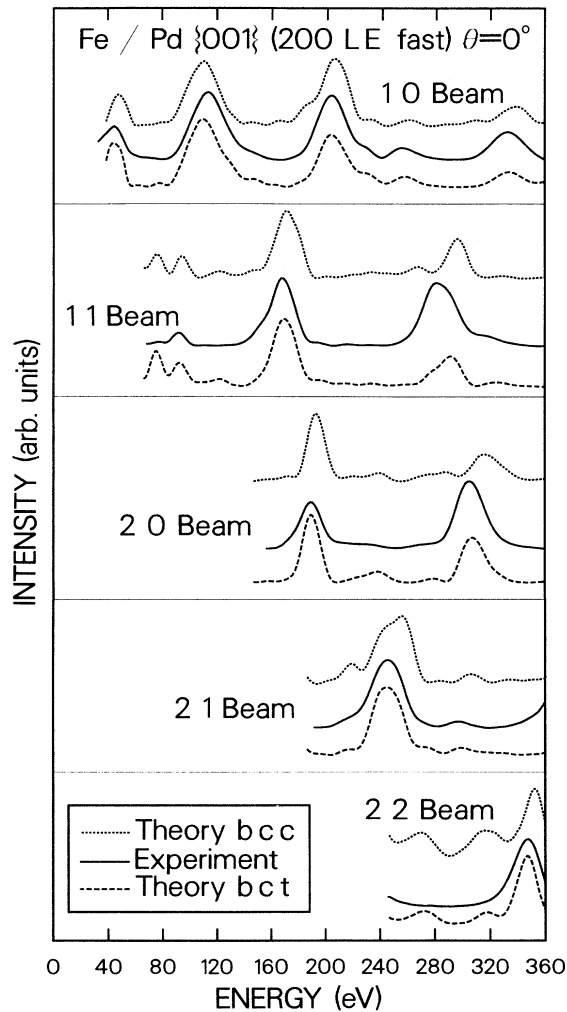


FIG. 6. Experimental and theoretical LEED spectra for a fast-grown 200-LE Fe film as described in the text. The dotted curves pertain to bcc Fe; the dashed curves to bct Fe as described in the text.

about 5.7 wt. % (more than twice the concentration found on the surface of the slowly grown films). How much the bulk concentration of carbon in these films was is not known, but we note that about 0.65 wt. % of carbon is reportedly sufficient to cause about 3% tetragonality in martensite.^{27,28}

Before closing this section on fast-grown thick films, it should be mentioned that we are not in a position to distinguish whether the change of the in-plane lattice constant was caused by the fast-growing rate or merely by the fact that the fast-grown films were much thicker than the slowly grown films (about 200 LE versus 65 LE).

IV. PHOTOEMISSION

The valence-band region of the Fe/Pd system was investigated by means of angle-resolved photoemission spectroscopy (ARPES). Electron distribution curves (EDC's) were monitored for normal emission with photon

energies varying between 28 and 100 eV and for different Fe coverages. Figure 7 (top) shows the EDC's measured with 62-eV photons. The valence-band spectrum of clean Pd{001} (curve marked 0) changes with increasing Fe coverage until a thickness of about 9 LE is reached, after which the emission from Pd disappears and the EDC's remain the same. Thus, these curves are descriptive of

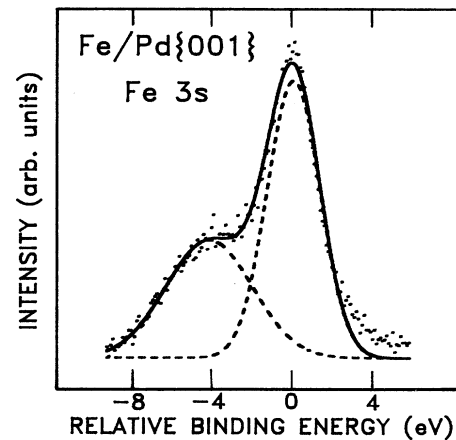
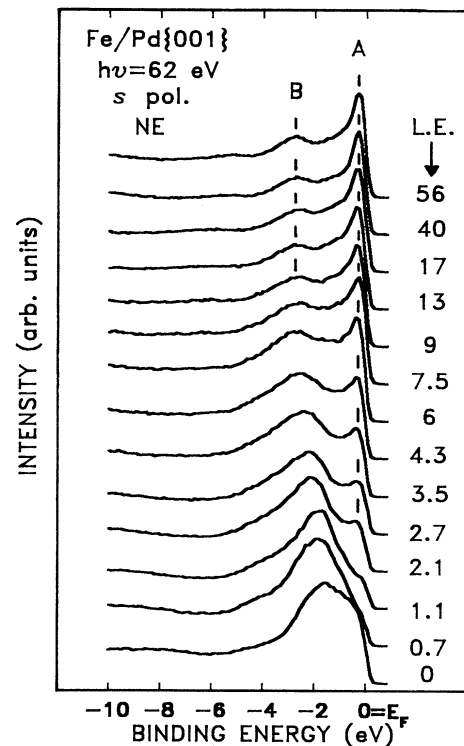


FIG. 7. Top: Normal-emission angle-resolved electron-distribution curves from epitaxial Fe films on Pd{001} with increasing thicknesses (values listed on the right, in LE). The incident synchrotron light was *s*-polarized with an energy of 62 eV. Bottom: Photoemission spectrum from the 3s core level in a 56-LE Fe film on Pd{001} as measured with 165-eV photons. The dots are experimental data (after background subtraction), the dashed curves are Gaussian fits to the data, and the solid curve is the sum of the two Gaussians.

the Fe film and are characterized by the presence of two peaks, marked *A* and *B* in the figure. Peak *A* (0.3 eV below the Fermi level) is due to the $\Gamma'_{25\downarrow}$ initial state and peak *B* (2.7 eV below the Fermi level) is due to the $\Gamma'_{25\uparrow}$ initial state.³⁵

The EDC's measured for thicknesses larger than about 9 LE are indistinguishable from those measured on thick Fe films grown on Ag{001} and proven to consist essentially of bcc Fe.¹⁴ In fact, the whole series of EDC's from thick Fe films on either Pd{001} or Ag{001} were found to be equal to one another, indicating that photoemission seems to be insensitive to the large distortion of the bcc Fe lattice as caused by the Pd{001} substrate. This result is in contrast with the observations made in the Cu/Pd{001} system, where the distortion caused by the pseudomorphism was reflected in dispersion characteristics different from those of the equilibrium phase.³⁶ It may be of interest, in this connection, to note that *no* *d*-band exchange splitting was observed³⁷ from fcc Fe on Cu{001}, a result attributed to the loss of ferromagnetic order.

The ferromagnetic properties of the thick Fe films grown on Pd{001} in this work are confirmed by the 3*s* core-level splitting. Figure 7 (bottom) depicts the photoemission spectrum of a 56-LE film measured with 165-eV photons. A two-Gaussian fit of the experimental data, after background subtraction, shows the split to be 4.2 eV with an accuracy estimated at 0.2 eV, corresponding to local magnetic moments of 1.9 μ_B (see Refs. 38 and 39). The published Fe 3*s* splittings are 4.5 eV for bulk bcc Fe,³⁸ 4.4 eV for one layer of Fe on Ag{001} (Ref. 40), 4.3 eV for 20-Å-thick Fe films on Cu{001} (Ref. 41), and ranging between 3.7 and 4.6 eV for Fe/Pd{111} with coverages between submonolayer to five layers.¹ Hence, assuming that the error bars in these literature values were the same as ours, we conclude that the Fe films grown in the present work exhibit the same 3*s* core-level splitting as either bcc or fcc Fe.

V. CONCLUSIONS

For deposition rates lower than about 0.5 Å/min, Fe grows pseudomorphically on Pd{001}, whether the substrate is left unheated at room temperature or cooled to about 120 K. The growth mode does not appear to be layer by layer, but rather appears to involve pseudomorphic epitaxial flat-topped {001} islands of unequal heights in the initial stages of growth.

The presence of steps and other defects between the islands causes the LEED pattern to deteriorate at coverages below 4–5 LE (layer equivalents), while the *I(V)* spectra change with respect to those of the clean substrate, owing to increasing contributions from the island terraces. This phenomenon is qualitatively similar to, but

quantitatively different from, that observed during the growth of Fe on Ag{001}.¹⁴ In the latter case, the *I(V)* spectra remain essentially identical to those of the clean substrate, and the LEED pattern almost disappears at coverages of 4–5 LE. Thus, in both cases, Fe on Ag{001} and Fe on Pd{001}, growth seems to occur initially by the nucleation of islands of ordered Fe atoms, but in the case of Fe/Ag{001} the islands have practically no large {001} or other surfaces (and hence do not contribute to the LEED signal), while in the case of Fe/Pd{001} the islands do have {001} surfaces that contribute to the LEED signal. This different behavior is puzzling, because the lattice misfit between Ag and Fe is very small (0.8%), whereas the misfit between Pd and Fe is rather large (4.1%). However, there is a larger gap between the surface free energies of Fe and Ag than between Fe and Pd (see Table II).

At higher coverages, Fe on Pd{001} keeps growing pseudomorphically if the growth rate is kept slow, and surprisingly thick films (at least 65 LE) can be grown despite the large lattice misfit (4.2%). The structure of these thick films is body-centered-tetragonal, and is a distortion of the stable bcc α -Fe caused by the planar epitaxial stress. The interlayer spacings in the surface region (and to a lesser extent the interlayer spacing in the bulk) undergo a gradual contraction with increasing thickness from 12 to about 40 LE. This rather uncommon phenomenon is not understood at the present time, but may possibly be due to a decrease of the magnetic moment in the surface region with increasing thickness of the film.

Very thick Fe films grown at a fast rate (of the order of 10 Å/min or more) are no longer pseudomorphic. Their structure is essentially the bcc structure of α -Fe, but with about 3% expansion of the bulk interlayer spacing in the direction perpendicular to the {001} surface. The origin of this expansion is not clear at this time, although it may be attributed speculatively to the presence of rather large concentrations of carbon unintentionally incorporated in the films during the growth process.

The photoemission results indicate that the thick films are ferromagnetic with a *d*-band exchange splitting of 2.4 eV and are electronically indistinguishable from either bulk bcc Fe, bcc Fe films grown on Ag{001}, or fcc Fe films grown on Cu{001}.

ACKNOWLEDGMENTS

We are grateful to John D. Myers (Battelle Columbus) for the Fe source used in the HL experiments. We are also indebted to the National Science Foundation and the Department of Energy for partial support of this work with Grants No. DMR-8709021 and No. DE-FG02-86ER45239, respectively.

¹C. Binns, C. Norris, G. P. Williams, M. G. Barthes, and H. A. Padmore, Phys. Rev. B **34**, 8221 (1986), and references cited therein.

²C. Liu and S. D. Bader, Physica B **161**, 253 (1989).

³C. Liu and S. D. Bader, in *Magnetic Properties of Low-Dimensional Systems II*, Vol. 50 of *Springer Proceedings in Physics*, edited by L. M. Falicov, F. Mejía-Lira, and J. L. Morán-López (Springer, Berlin, 1990), p. 22.

- ⁴D. Tian, S. C. Wu, F. Jona, and P. M. Marcus, *Solid State Commun.* **70**, 199 (1989).
- ⁵F. Jona, J. A. Strozier, Jr., and P. M. Marcus, in *Structure of Surfaces*, edited by M. A. Van Hove and S. Y. Tong (Springer, Berlin, 1985), p. 92.
- ⁶Y. Dai, H. Li, and F. Jona, *Rev. Sci. Instrum.* **61**, 1724 (1990).
- ⁷L. E. Davis, N. C. MacDonald, P. W. Palmberg, G. E. Riach, and R. E. Weber, *Handbook of Auger Electron Spectroscopy* (Physical Electronic Industries, Inc., Eden Prairie, Minnesota, 1978).
- ⁸S. Tanuma, C. S. Powell, and D. R. Penn, *Surf. Sci.* **192**, L849 (1987).
- ⁹W. F. Egelhoff, Jr. and I. Jacob, *Phys. Rev. Lett.* **62**, 921 (1989), and references cited therein.
- ¹⁰D. K. Flynn, W. Wang, S. L. Chang, M. C. Tringides, and P. A. Thiel, *Langmuir* **4**, 1096 (1988); D. K. Flynn, J. W. Evans, and P. A. Thiel, *J. Vac. Sci. Technol. A* **7**, 2162 (1989).
- ¹¹H. D. Shih, F. Jona, D. W. Jepsen, and P. M. Marcus, *Phys. Rev. B* **15**, 5550 (1977).
- ¹²E. Bauer and J. H. van der Merwe, *Phys. Rev. B* **33**, 3657 (1986).
- ¹³N. Hosoi, T. Shinjo, and T. Takada, *J. Phys. Soc. Jpn.* **50**, 1903 (1981).
- ¹⁴H. Li, Y. S. Li, J. Quinn, D. Tian, J. Sokolov, F. Jona, and P. M. Marcus, *Phys. Rev. B* **42**, 9195 (1990).
- ¹⁵D. W. Jepsen, *Phys. Rev. B* **22**, 5701 (1980); **22**, 814 (1980).
- ¹⁶V. L. Moruzzi, J. F. Janak, and A. R. Williams, *Calculations of Electronic Properties of Metals* (Pergamon, New York, 1978).
- ¹⁷M. A. Van Hove, S. Y. Tong, and M. H. Elconin, *Surf. Sci.* **64**, 85 (1977).
- ¹⁸J. B. Pendry, *J. Phys. C* **13**, 937 (1980).
- ¹⁹E. Zanazzi and F. Jona, *Surf. Sci.* **62**, 61 (1977).
- ²⁰F. Jona and P. M. Marcus, *Surf. Sci.* **223**, L897 (1989).
- ²¹W. B. Pearson, *A Handbook of Lattice Spacings and Structures of Metals and Alloys* (Pergamon, New York, 1967), Vol. 2.
- ²²G. Simmons and H. Wang, *Single Crystal Elastic Constants and Calculated Aggregate Properties: A Handbook*, 2nd ed. (MIT Press, Cambridge, 1971).
- ²³S. H. Lu, J. Quinn, D. Tian, F. Jona, and P. M. Marcus, *Surf. Sci.* **209**, 364 (1989).
- ²⁴V. L. Moruzzi and P. M. Marcus, *Phys. Rev. B* **39**, 471 (1989).
- ²⁵R. Richter, J. G. Gay, and J. J. Smith, *J. Vac. Sci. Technol. A* **3**, 1498 (1985); *Phys. Rev. Lett.* **54**, 2704 (1985).
- ²⁶C. L. Fu, A. J. Freeman, and T. Oguchi, *Phys. Rev. Lett.* **54**, 2700 (1985).
- ²⁷C. S. Roberts, *Trans. AIME (J. Met.)* **197**, 203 (1953).
- ²⁸M. A. Shtremel', L. M. Kaputkina, S. D. Prokoshkin, and Yu. A. Krupin, *Fiz. Met. Metalloved. (USSR)* **57**, 1222 (1984) [*Phys. Met. Metall.* **57**, 168 (1984)].
- ²⁹M. P. Seah and W. A. Dench, *Surf. Int. Anal.* **1**, 2 (1979); see formula (5) and Table I.
- ³⁰C. Liu and S. D. Bader (private communication).
- ³¹C. M. Schneider, J. J. de Miguel, P. Bressler, J. Garbe, S. Ferrer, R. Miranda, and J. Kirschner, *J. Phys. (Paris) Colloq.* **49**, C8-1657 (1988).
- ³²L. Z. Mezey and J. Giber, *Jpn. J. Appl. Phys.* **21**, 1569 (1982).
- ³³W. R. Tyson and W. A. Miller, *Surf. Sci.* **62**, 267 (1977).
- ³⁴A. R. Miedema, P. F. de Châtel, and F. R. de Boer, *Physica B + C* **100B**, 1 (1980).
- ³⁵E. Kisker, K. Schröder, W. Gudat, and M. Campagna, *Phys. Rev. B* **31**, 329 (1985).
- ³⁶H. Li, S. C. Wu, D. Tian, J. Quinn, Y. S. Li, F. Jona, and P. M. Marcus, in *The Structure of Surfaces III*, edited by S. Y. Tong (Springer, New York, in press).
- ³⁷A. A. Hezaveh, G. Jennings, D. Pescia, and R. F. Willis, *Solid State Commun.* **57**, 329 (1986).
- ³⁸D. J. Joyner, O. Johnson, and D. M. Hercules, *J. Phys. F* **10**, 169 (1980).
- ³⁹D. A. Shirley, in *Photoemission in Solids I*, edited by M. Cardona and L. Ley (Springer, Berlin, 1978), p. 165.
- ⁴⁰C. Binns, P. C. Stephenson, C. Norris, G. C. Smith, H. A. Padmore, G. P. Williams, and M. G. Barthes-Labrousse, *Surf. Sci.* **152/153**, 237 (1985).
- ⁴¹H. I. Starnberg, M. T. Johnson, D. Pescia, and H. P. Hughes, *Surf. Sci.* **178**, 336 (1986).